JCTC Journal of Chemical Theory and Computation

Elucidation of Rate Variations for a Diels−Alder Reaction in Ionic Liquids from QM/MM Simulations

Orlando Acevedo,[†] William L. Jorgensen,*[,†] and Jeffrey D. Evanseck*[,‡]

Department of Chemistry, Yale University, 225 Prospect Street, New Haven, Connecticut 06520-8107, and Center for Computational Sciences and Department of Chemistry and Biochemistry, Duquesne University, Pittsburgh, Pennsylvania 15282-1530

Received August 25, 2006

Abstract: The impact of acidic and basic ionic liquid 1-ethyl-3-methylimidazolium chloride (EMIC) melts upon cyclopentadiene and methyl acrylate Diels−Alder reaction rates has been investigated using QM/MM calculations. The ability of the ionic liquid to act as a hydrogen bond donor (cation effect), moderated by its hydrogen bond accepting ability (anion effect), has been proposed previously to explain observed *endo/exo* ratios. However, the molecular factors that endow ionic liquids with their rate enhancing potential remain unknown. New OPLS-AA force field parameters in conjunction with potentials of mean force (PMF) derived from free energy perturbation calculations in Monte Carlo simulations (MC/FEP) are used to compute activation energies. QM/MM simulations using a periodic box of ions reproduce relative rate enhancements for the EMIC melts compared to water and 1-chlorobutane that reproduce kinetic experiments. Solute−solvent interactions in acidic and basic ionic liquid melts have been analyzed at key stationary points along the reaction coordinate. The reaction rate was found to be greater in the acidic rather than the basic melt due to less-dominant ion-pairing in the acidic melt, enabling the EMI cation to better coordinate to the dienophile at the transition state. The simulations suggest that the hydrogen on C2 of the EMI cation does not contribute to stabilization of the transition state, as previously believed, and the interactions with the more sterically exposed hydrogens on C4 and C5 play a larger role. In addition, the relative stabilization of the transition state through electrostatic interactions with the EMI cation in the acidic melt is also greater than that afforded by the weaker Lewis-acid effect provided by hydrogen bonding with water molecules in aqueous solution.

Introduction

Though the observed effects of ionic liquids on chemical reactions range from weak to powerful,[1] only a few systematic studies have addressed the microscopic details on how ionic liquids influence chemical reactivity and selectivity.[2−5] Large rate accelerations and stereoselectivity enhancements have been observed for the Diels−Alder reaction between cyclopentadiene and methyl acrylate in the ionic liquid 1-ethyl-3-methylimidazolium chloride (EMIC) (Scheme 1) when compared to common organic solvents or water.[6−8] The mechanism behind the ionic liquid's impact on the reaction is not well understood, although high internal solvent pressure,[9] hydrogen bonding,[3,5] solvent polarity,[10] and Lewis acidity[11] are thought to contribute to the phenomena. Rate enhancements in ionic liquids also differ depending on the counteranion, i.e., BF_4^-, PF_6^-, ClO_4^-, and, of particular interest, the chloroaluminates from $AlCl_3$.[6,7,12]

An attractive property of using $AlCl_3$ is that the Lewis acidity of the melt can be varied with the composition of the liquid.[13] Raman,[14] ^{27}Al NMR,[15] and mass spectra[16] all indicate that when $AlCl_3$ comprises <50% mol of the EMIC

* Corresponding authors e-mail: evanseck@duq.edu (J.D.E.) and william.jorgensen@yale.edu (W.L.J).

[†] Yale University.

[‡] Duquesne University.

10.1021/ct6002753 CCC: $37.00
Published on Web 11/15/2006

Scheme 1. Diels−Alder Reaction between Cyclopentadiene and Methyl Acrylate Giving *Endo* and *Exo* Bicyclic Products in 1-Ethyl-3-methylimidazolium Chloride (EMIC) Solvent

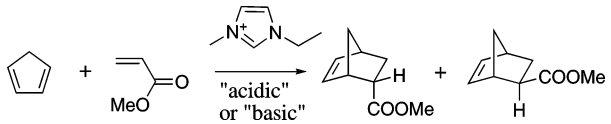

ionic liquid melt, $AlCl_4^-$ is the only chloroaluminate species present. These "basic melts" are composed of EMI^+, $AlCl_4^-$, and with chloride ions that are not bound to aluminum. A ratio >1:1 $AlCl_3$ to EMIC is referred to as an "acidic melt"; ^{27}Al NMR[17] and negative-ion FAB mass spectra[18] have shown that $AlCl_4^-$ and $Al_2Cl_7^-$ are the principal anionic constituents in this case.

When an acidic melt (51% $AlCl_3$) of EMIC was used as the solvent for the Diels−Alder reaction in Scheme 1, the experimental rate of reaction was 10, 175, and 560 times faster than in water, ethyl ammonium nitrate, and 1-chlorobutane, respectively.[6] However, the basic melt (48% $AlCl_3$) of EMIC gave a rate 2.4 times slower than that of water. *Endo* selectivity is also enhanced with good yield when using an acidic EMIC ionic liquid. A 6.7:1 *endo*/*exo* ratio is observed for the solvent ethyl ammonium nitrate (EAN), the basic ionic liquid EMIC melt has a ratio of 5.25:1, while the acidic melt ionic liquid EMIC has a ratio of 19:1; typical nonpolar solvents have *endo/exo* selectivities of 2:1.[6,19]

Welton and co-workers have recently proposed that selectivity enhancements for the reaction between cyclopentadiene and methyl acrylate in a variety of ionic liquids result from a competition between the anion and the dienophile at the transition state for hydrogen bonding [The term hydrogen bonding is used throughout the ionic liquid literature and used in this study as well, despite the fact that the classical definition of a hydrogen bond is not formally followed.] with the cation.[3] Hence, the highest selectivities come from ionic liquids with the strongest hydrogen-bond donor capacity, along with the weakest hydrogen-bond acceptor ability.[3,5] The suggestion has been made that hydrogen bonding may also dictate the rate acceleration, since the increased rate is observed to be concurrent with increased *endo*-selectivity.[3] However, since the correlation is qualitative and does not consider other effects influencing the rate of reaction, a detailed study is necessary to elucidate the intermolecular interactions occurring at the transition state.

To investigate the dramatic kinetic effects of ionic liquids at the atomic level, mixed quantum and molecular mechanical (QM/MM) simulations have been carried out on the Diels−Alder reaction in solution with complete sampling of the geometry of the reacting systems and explicit representation of the solvent components. Reactants, transition structures, and products have been located using force fields in four solvents: acidic and basic chloroaluminate ionic liquids, water, and 1-chlorobutane. The present results indicate that the lowering of the activation barrier does feature enhanced interactions between EMI^+ and the transition state in the acidic melt, but the previously suggested hydrogen bonding with the hydrogen on C2 of EMI^+ is not apparent.[3,4] This investigation provides an understanding of the intermolecular short- and long-range interactions occurring during the reaction, and it sheds light on how to optimize ionic liquids to control other organic reactions.

Computational Methods

Mixed quantum and molecular mechanical (QM/MM) calculations,[20] as implemented in BOSS 4.6[21] were carried out with the reacting system treated with the PDDG/PM3 method.[22] PDDG/PM3 is a semiempirical QM method that has been extensively tested for gas-phase structures and energetics[22] and has given excellent results in solution-phase QM/MM studies of S_N2 reactions,[23] nucleophilic aromatic substitution reactions,[24] decarboxylations,[25,26] and Cope eliminations.[27] The solvent molecules were represented with the TIP4P water model,[28] the all-atom OPLS force field for 1-chlorobutane,[29] and newly developed OPLS parameters for the ionic liquids.[30−32] Binary solvent boxes containing 384 molecules were constructed for model acidic (192 EMI^+ and 192 $Al_2Cl_7^-$ ions) and basic melts (192 EMI^+ and 192 $AlCl_4^-$ ions) and equilibrated for 80M and 65M configurations, respectively. Periodic boundary conditions were used, and the dimensions of the simulation cells were ca. 42 × 42 × 62 Å and 38 × 38 × 56 Å for the acidic and basic melts, respectively. Binary solvent media were also used in the technically similar study for decarboxylation of a biotin model.[26] Partial charges for the ionic liquid cation and anions were obtained from B3LYP/6-31G(d) calculations with the CHELPG method.[33] The EMI cation had full bond and angle flexibility, and torsion angle sampling was included for the ethyl side chain. The anions were kept internally rigid throughout the simulations. Solute−solvent and solvent−solvent intermolecular cutoff distances of 12 Å were employed for the reaction in water based roughly on center-of-mass separations. A feathering of the intermolecular interactions within 0.5 Å of the cutoff is applied. Long-range electrostatics were treated with the Ewald method for the ionic liquids and 1-chlorobutane. In short, Ewald summations calculate the exact electrostatic energy of an infinite lattice of identical copies of the simulation cell. This suppresses artifacts resulting from the simple cutoff of the long-range electrostatic interactions prevalent in the ionic liquid. Total translations and rotations were sampled in ranges that led to overall acceptance rates of about 45% for new configurations.

Free energy perturbation (FEP) calculations were performed in conjunction with Metropolis Monte Carlo (MC) simulations in the NPT ensemble at 25 °C and 1 atm. In this QM/MM implementation, the solutes are treated quantum mechanically using PDDG/PM3; computation of the QM energy and atomic charges was performed for every attempted solute move, occurring every 100 configurations. Electrostatic contributions to the solute−solvent energy were calculated using CM3 charges,[34] with a scale factor of 1.08. The initial geometry of the reacting system was obtained from density functional theory calculations, and the *endo*-cis addition mode was chosen in all cases. FEP windows were run simultaneously using multiple processors on Pentium-based clusters located at Yale University and the Center for Computational Sciences (CCS) at Duquesne University.

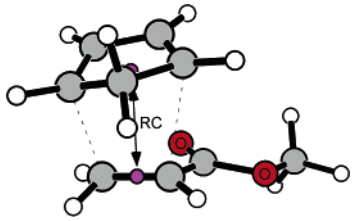

Figure 1. Reaction coordinate, RC, for the Diels−Alder reaction is defined as the distance between the midpoints of the C═C bond of the dienophile and the diene's terminal carbons. The transition structure from gas-phase B3LYP/6-31G(d) calculations is illustrated.

Results and Discussion

Force Field for the Ionic Liquids. To elucidate the effect of the room-temperature ionic liquid EMIC on the Diels−Alder reaction, a custom force field has been parametrized to model EMIC acidic and basic melts. Recent theoretical work has been reported on force the field development for several ionic liquids.[30,35] Parameters specific to the current EMIC-$AlCl_3$ ionic liquid have been created starting from a force field developed and validated by Lopes et al.[30] from existing OPLS-AA parameters designed for heterocyclic aromatic rings.[31] Lennard-Jones parameters for Cl atoms have been fit to the Born-Mayer potential used to describe dispersive interactions in molten salts.[30] Improvements to the Lopes et al. force field specific to EMIC-$AlCl_3$ have been achieved by using new equilibrium bond lengths and angles based on the B3LYP/6-31G(d) geometries, new partial charges computed with the CHELPG method and B3LYP/6-31G(d), and new torsion potentials for the side-chain rotation of the ethyl group in the EMI cation (see the Supporting Information). Computed densities of 1.22 and 1.20 g/cm^3 for the acidic and basic melt, respectively, agree well with the experimental value of 1.266 g/cm^3 at 60 °C for the 1:1 melt.[36] Further validation of the force field including radial pair distributions, g(r), can be found in references by Lopes et al.[30] and de Andrade et al.[35b] which used similar setups and parameters. Complete force field parameters are reported in the Supporting Information.

Table 1. Free Energy Changes (kcal/mol) at 25 °C for the Diels−Alder Reaction between Cyclopentadiene and Methyl Acrylate from QM/MM/MC Simulations

	water	acidic melt	basic melt	BuCl
$\Delta G^{\ddagger}$ (calc)[a]	42.9	40.0	43.5	43.8
$\Delta\Delta G^{\ddagger}$ (calc)	0.0	−2.9	0.6	0.9
$\Delta\Delta G^{\ddagger}$ (exptl)[b]	0.0	−1.36	0.52	2.39

[a] Statistical uncertainties (1σ) are ±0.4 kcal/mol. [b] Reference 6.

Energetics and Structure. Free-energy profiles for the Diels−Alder reaction have been calculated by perturbing a reaction coordinate (RC) defined by the distance between two dummy atoms located at the midpoint of the diene terminal carbon atoms and the midpoint of the dienophile C═C bond, as shown in Figure 1. The range of RC spanned is from 1.42 to 4.20 Å with an increment of 0.02 Å. Each FEP calculation entailed between 5 and 35 million (M) configurations of equilibration followed by 10 M configurations of averaging. The number of single-point QM calculations required for one free energy profile is 20−80 million, clearly showing the need for highly efficient QM methods in such studies. The computed free energy profiles for the reaction in water and in acidic and basic EMIC are shown in Figure 2.

The cycloadduct minimum is found when RC is close to 1.5 Å, while the transition state occurs around 2.12 Å in all solvent systems. The Diels−Alder mechanism was found to be concerted in chloroaluminate ionic liquids, which agrees with previous density functional theory calculations.[4] The free energies are relatively constant for RC beyond 4 Å. The differential solvent effects can be seen primarily near the transition state. The principal point is that the QM/MM/MC approach qualitatively reproduces the observed rate acceleration by acidic ionic liquids and the rate retardation by basic ionic liquids for the Diels−Alder reaction in comparison to aqueous solution. The computed and experimental $\Delta\Delta G^{\ddagger}$ values for the acidic melt are −2.9 and −1.4 kcal/mol, while

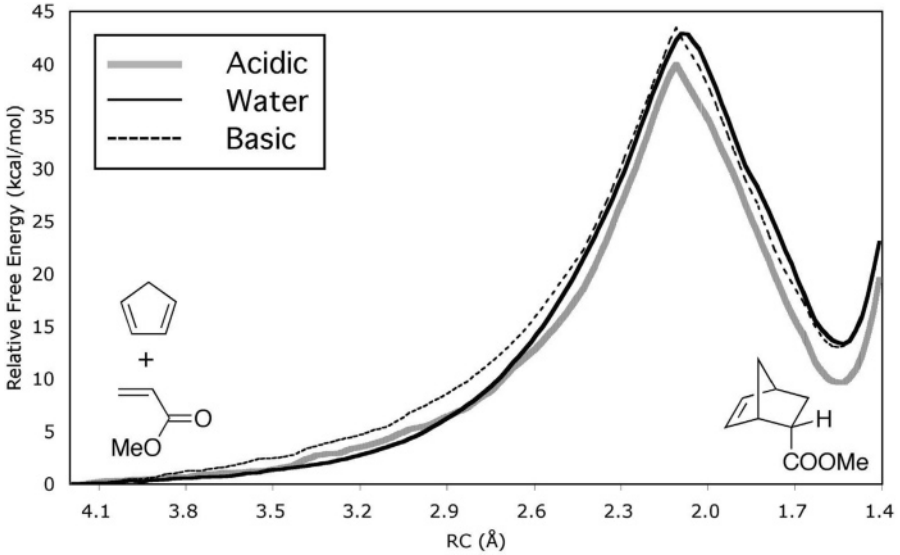

Figure 2. Computed free energy profiles in acidic and basic ionic liquids and water for the cycloaddition between cyclopentadiene and methyl acrylate.

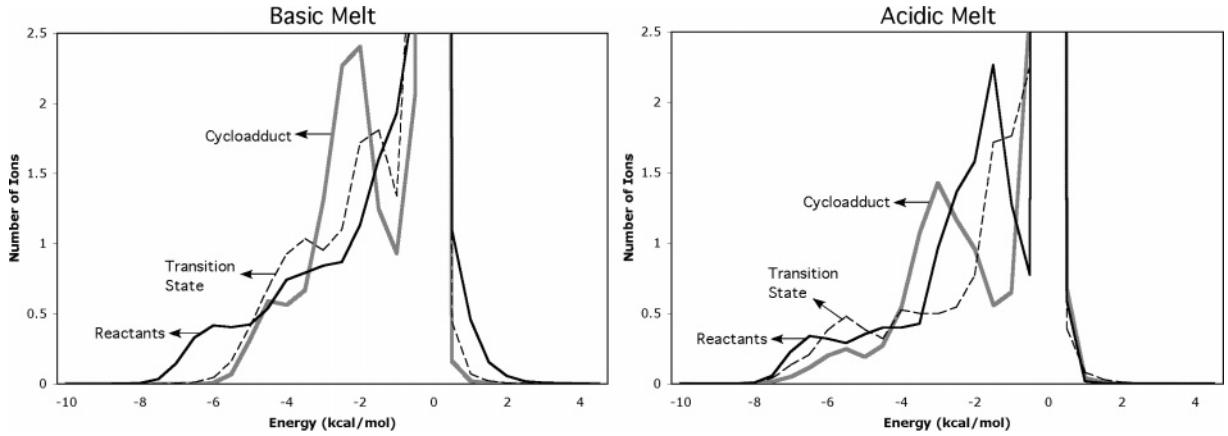

Figure 3. Solute−solvent energy pair distributions for the reaction of cyclopentadiene with methyl acrylate for structures near the reactants, transition state, and product. The ordinate records the number of ions in the melts that interact with the solutes with their interaction energy on the abscissa. Units for the ordinate are number of ions per kcal/mol.

they are 0.6 and 0.52 kcal/mol for the basic melt (Table 1). Since the same computational approach is used for all solvents, most errors are expected to cancel. The computed $\Delta\Delta G^{\ddagger}$ values reproduce well the rate enhancement differences between the basic and acidic melts. Exact agreement could not be expected since the ionic composition of the experimental and modeled systems is not identical.

Uncertainties in the free energy barriers have been calculated by propagating the standard deviation (σ_i) on each individual ΔG_i.[21] Smooth free energy profiles were obtained with statistical uncertainties ($1\sigma_i$) of only 0.005−0.06 kcal/mol in each window; the overall uncertainties have been computed using the equation $\sqrt{\sum_i^N \sigma_i^2}$, where N is the number of ΔG_i values. The computed errors in the free energies of activation, $\Delta G^{\ddagger}$, for water and both ionic liquid melts are computed to be ± 0.4 kcal/mol. For the $\Delta\Delta G^{\ddagger}$ calculations, the propagation of errors through variances is not explicit and cannot be used to compute uncertainties in the relative barriers.

The free energy profile for the Diels−Alder reaction was subsequently also computed in 1-chlorobutane. Before the reaction was modeled, pure liquid properties were also checked through MC simulations. A periodic box of 384 fully flexible 1-chlorobutane molecules was created and equilibrated for 20 M and then averaged for 10 M configurations. The computed heat of vaporization of 7.28 kcal/mol (exptl = 7.26 kcal/mol)[37] and density of 0.83 g/cm^3 (exptl = 0.886 g/cm^3)[38] are both in good accord with experiment. The $\Delta G^{\ddagger}$ of 1-chlorobutane was then computed to be 43.8 kcal/mol (Table 1). The increase relative to the acidic melt is 3.8 kcal/mol, which is in excellent agreement with the experimental result of 3.75 kcal/mol.[6] A plot of the free energy profile in 1-chlorobutane can be found in the Supporting Information.

Although the relative free energies of activation are in good agreement with experiment, the absolute values are overestimated. The experimental $\Delta G^{\ddagger}$ reported for the Diels−Alder reaction in a 50/50 methanol/water mixture was 22.4 kcal/mol.[39] The $\Delta G^{\ddagger}$ values for the ionic liquids should be reasonably close to the water mixture (±2 kcal/mol), so the 40−43 kcal/mol values from PDDG/PM3 are too high. This has been noted for other Diels−Alder reactions,[22] and in previous QM/MM/MC work on aqueous-phase Diels−Alder reactions involving cyclopentadiene and three different dienophiles (acyrlonitrile, methyl vinyl ketone, and 1,4-naphthoquinone), the AM1 semiempirical method also overestimated the absolute activation energies, while leading to good relative values.[40] As noted, computation of each QM/MM/MC free energy profile entailed ca. 20−80 million QM calculations, which make the use of far more computationally taxing ab initio or DFT methods prohibitive from a practical standpoint.

Solvation. The close agreement between the computed and observed changes in free energies of activations (Table 1) indicates that the QM/MM/MC simulations capture the origins of the medium effects at the molecular level. Differential stabilization of the transition structure through hydrogen bonding may be the primary factor affecting the rate, as found in prior simulations of Diels−Alder reactions in water.[40,41] In order to elucidate the differences between the acidic and basic melts, the interaction energies for both were quantified by analyzing the solute−solvent energy pair distributions from QM/MM/MC calculations in three representative FEP windows: near the reactants, transition state, and product. The distributions record the average number of ions in the ionic liquids that interact with the reacting system and their corresponding energies. Very favorable interaction energies between solute and solvent components are reflected in the left-most region with energies more attractive than ca. −5 kcal/mol (Figure 3). The large band near 0 kcal/mol arises from the many ions in outer shells.

In viewing Figure 3, the reactants appear to have similar distributions for both acidic and basic melts leading to comparable ground-state stabilization in both ionic liquids. Integration of the distributions for the reactants from −10.0 to −5.0 kcal/mol confirms the similar number of very favorable interactions (Table 2). However, the distribution for the transition states is clearly different with a larger number of very favorable interactions in the acidic melt (Table 2). Specifically, the number of interactions in the −10 to −5 kcal/mol range decreases by about one in going from the reactants to transition state in the basic melt; however, in the acidic melt, the same number of interactions is retained.

Table 2. Number of Solute−Solvent Interactions for the Reactants, Transition State, and Product Integrating from −10.0 to −5.0 kcal/mol from QM/MM/MC Simulations

	reactants	transition state	cycloadduct
basic	1.8	0.6	0.4
acidic	1.6	1.6	0.8

In addition, there is a shift in the average strength of the most favorable interactions to lower energy by about 2 kcal/mol (Figure 3). The pattern is fully consistent with the faster reaction rate in the acidic melt.

The exact nature of these most favorable solute-ion interactions is of obviously relevant interest. Figure 4 shows snapshots of the transition structures in the acidic and basic melts from the QM/MM/MC simulations. Immediately a major difference in the structure compared to that expected from chemical intuition is observed. For both the acidic and basic melts, hydrogen bonds are not observed between HC2 of the EMI cation and the dienophile's carbonyl group. In the basic melt, the HC2 unit is shielded by the adjacent methyl and ethyl groups and also represents a small volume element. The anions congregate around the diene forming electrostatically favorable interactions with hydrogens, while two EMI cations complex near the carbonyl oxygen of the dienophile. This partitioning of the ions is consistent with the direction of the dipole for the transition state. In the acidic melt, an EMI ring hydrogen makes a short contact with the carbonyl oxygen, while only the methyl and ethyl groups of the two cations are the most proximal in the basic melt. As noted previously,[40−43] hydrogen bonding is sensitive to small charge shifts. In the present case, charges were computed from the final transition state configuration sampled (Figure 4) which is a good representation of the average structure.[40] On the carbonyl oxygen of the methyl acrylate reactant, the charge only declines from −0.288 and −0.291 e in the acidic and basic melt, respectively, to −0.322 and −0.313 e in the transition state (Table 3). However, the charge computed on the carbonyl carbon in the acidic melt *increases* from +0.475 to +0.501 e from reactant to transition structure, while *decreasing* from +0.491 to 0.466 e in the basic melt (Table 3). Thus, the Diels−Alder transition state in the acidic melt has the greatest C^{+}—O^{-} polarization. This is consistent with enhanced hydrogen bonding in the acidic melt and a reduced activation barrier as compared to the basic melt.

Table 3. CM3 Charges for the Carbonyl Oxygen and Carbon on Methyl Acrylate in the Basic and Acidic Melts for the Diels−Alder Reactants, Transition Structure, and Cycloadduct Using PDDG/PM3

	carbonyl O	carbonyl C
	Basic	
reactants	−0.291	0.491
transition state	−0.313	0.466
cycloadduct	−0.339	0.472
	Acidic	
reactants	−0.288	0.475
transition state	−0.322	0.501
cycloadduct	−0.342	0.473

Previous work has shown that the presence of hydrogen-bond donors in the reaction medium leads to enhanced *endo:exo* selectivities Diels−Alder reactions.[3,5,7] This finding has Aggarwal et al. to suggest that the most likely complex determining the selectivity in ionic liquids involves the most acidic proton (HC2) of the EMI cation interacting with the carbonyl oxygen of the dienophile.[3] However, higher selectivities have been observed in 1-alkyl,2,3-dimethylimidazolium ionic liquids, where the 2-position hydrogen has been replaced with a methyl group.[5] The results suggest that the hydrogen-bond donor properties for HC2 of the cation do not exclusively account for the strong *endo* selectivities observed and that other interactions, e.g., with hydrogens on C4 and C5, may play a larger role. The latter hydrogens

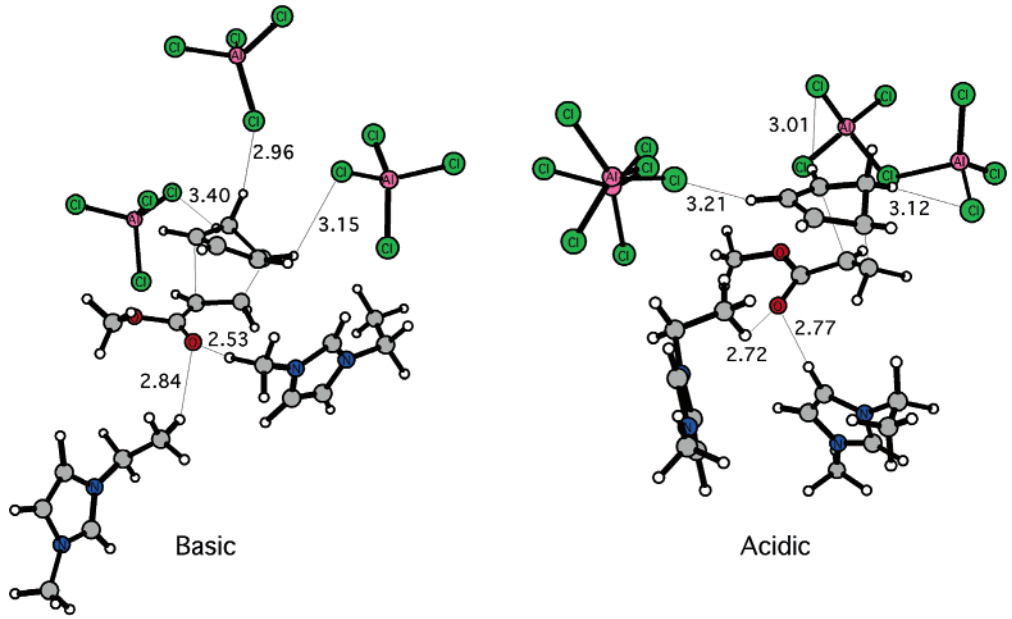

Figure 4. Typical snapshots of transition structures for the Diels−Alder reaction in the basic and acidic melts (only the nearest ions are illustrated). The distances (in Å) are average values over the final 10 million configurations of QM/MM/MC simulations.

are more sterically accessible, and their partial charges are essentially the same as for HC2 (see the Supporting Information). The present computations indicate that the HC2 fragment of the EMI cation is, in fact, not involved in hydrogen bonding with the dienophile at the transition state. The ions in the ionic liquids form ion-pairs with large binding energies, as shown by the DFT calculations,[4] and the interactions weaken gradually as the melt becomes more acidic. Consistently, the acidic melt exhibits enhanced hydrogen bonding with the transition structure, since the energetics of ion-pairing are less dominant; the more acidic hydrogens in the EMI ring are then less engaged in the ion pairing. The basic melt, featuring stronger ion-pairing interactions, prefers to have the ring hydrogens interacting with nearby $AlCl_4^-$ anions allowing only weaker solvation of the transition state through interactions with the methyl and ethyl groups of EMI^+.

In summary, the qualitative picture that emerges is that the reaction rate is greater in the acidic rather than the basic melt because ion-pairing is less dominant in the acidic melt, which enables the EMI cations to better coordinate with the dienophile at the transition state; the coordination does feature hydrogen bonding with the dienophile's carbonyl oxygen, but it is with the more sterically exposed hydrogens on C4 and C5 of the cation rather than the hydrogen on C2. The relative stabilization of the transition state through hydrogen bonding with the EMI cation in the acidic melt is also greater than that afforded by the weaker Lewis-acid effect afforded by hydrogen bonding with water molecules in aqueous solution.[40−42,44]

Conclusions

QM/MM/MC simulations have been carried out for the Diels−Alder reaction in ionic liquids, water, and 1-chlorobutane in good agreement with kinetic experiments. Analysis of the explicit solute−solvent interactions at the transition state indicates that an enhanced coordination of hydrogen bonds at the carbonyl oxygen is largely responsible for the reaction rate being greater in the acidic rather than the basic melt. The rate enhancements in the acidic melt arise from preferential hydrogen bonding with the more sterically exposed C4 and C5 hydrogens on the EMI cation rather than the hydrogen on C2. Strong ion-pairing in the basic melt prevents the ring hydrogens from participating at the transition state. In aqueous solution, a weaker Lewis-acid effect is provided by hydrogen bonding with water molecules compared to the EMI cations in the acidic melt. The findings have a significant impact for predicting the effect of ionic liquids on other organic reactions; improvements in rate are expected to be limited in the absence of differential hydrogen bond stabilization of the transition state.

Acknowledgment. J.D.E. is grateful to the NSF (CHE-0321147, CHE-0354052, AAB/PSC CHE-030008P), Department of Education (P116Z040100 and P116Z050331), and SGI Corporation for the support of this work. Support at Yale was provided by the NSF CHE-0130996.

Supporting Information Available: OPLS-AA force field parameters for EMIC-$AlCl_3$, free energy profile in 1-chlorobutane, DFT energies, zero-point energies, imaginary frequencies, and Cartesian coordinates of all structures. This information is available free of charge via the Internet at http://pubs.acs.org.

References

(1) (a) Seddon, K. R. *J. Chem. Technol. Biotechnol.* **1997**, *68*, 351−356. (b) Welton, T. *Chem. Rev.* **1999**, *99*, 2071−2083. (c) Wasserscheid, P.; Keim, W. *Angew. Chem. Int. Ed.* **2000**, *39*, 3772−3789. (d) Jain, N.; Kumar, A.; Chauhan, S.; Chauhan, S. M. S. *Tetrahedron* **2005**, *61*, 1015−1060.

(2) (a) Bock, C. W.; Trachtman, M.; Mains, G. J. *J. Phys. Chem.* **1994**, *98*, 478−485. (b) Hébant, P.; Picard, G. *J. Mol. Struct. (Theochem)* **1995**, *358*, 39−50. (c) Picard, G.; Bouyer, F. C.; Leroy, M.; Bertaud, Y.; Bouvet, S. *J. Mol. Struct. (Theochem)* **1996**, *368*, 67−80. (d) Takahashi, S.; Suzuya, K.; Kohara, S.; Koura, N.; Curtiss, L. A.; Saboungi, M. L. *Z. Phys. Chem.* **1999**, 209−222.

(3) Aggarwal, A.; Lancaster, N. L.; Sethi, A. R.; Welton, T. *Green Chem.* **2002**, *4*, 517−520.

(4) Acevedo, O.; Evanseck, J. D. In *Ionic Liquids as Green Solvents: Progress and Prospects*; ACS Symposium Series, 2003; Vol. 856, pp 174−190.

(5) Vidis, A.; Ohlin, C. A.; Laurenczy, G.; Küsters, E.; Sedelmeier, G.; Dyson, P. J. *Adv. Synth. Catal.* **2005**, *347*, 266−274.

(6) Lee, C. W. *Tetrahedron Lett.* **1999**, *40*, 2461−2464.

(7) Fischer, T.; Sethi, A.; Welton, T.; Woolf, J. *Tetrahedron Lett.* **1999**, *40*, 793−796.

(8) (a) Kumar, A.; Pawar, S. S. *J. Org. Chem.* **2004**, *69*, 1419−1420. (b) Kumar, A.; Pawar, S. S. *J. Mol. Catal. A: Chem.* **2004**, *208*, 33−37. (c) Tiwari, S.; Kumar, A. *Angew. Chem. Int. Ed.* **2006**, *45*, 4824−4825.

(9) Eldik, R. V.; Asano, T.; Le, Noble, W. *Chem. Rev.* **1989**, *89*, 549−688.

(10) Berson, J. A.; Hamlet, Z.; Mueller, W. A. *J. Am. Chem. Soc.* **1962**, *84*, 297−304.

(11) Otto, S.; Blokzijl, W.; Engberts, J. B. F. N. *J. Org. Chem.* **1994**, *59*, 5372−5376.

(12) Earle, M. J.; McCormac, P. B.; Seddon, K. R. *Green Chem.* **1999**, *1*, 23−25.

(13) Hussey, C. L. *Pure Appl. Chem.* **1988**, *60*, 1763−1772.

(14) Gale, R. J.; Gilbert, B. P.; Osteryoung, R. A. *Inorg. Chem.* **1978**, *17*, 2728−2729.

(15) Wilkes, J. S.; Frye, J. S.; Reynolds, G. F. *Inorg. Chem.* **1983**, *22*, 3870−3872.

(16) (a) Ackermann, B. L.; Tsarbopoulos, A.; Allison, J. *Anal. Chem.* **1985**, *57*, 1766−1768. (b) Wicelinski, S. P.; Gale, R. J.; Pamidimukkala, K. M.; Laine, R. A. *Anal. Chem.* **1988**, *60*, 2228−2232.

(17) Gray, J. L.; Maciel, G. E. *J. Am. Chem. Soc.* **1981**, *103*, 7147−7151.

(18) Franzen, G.; Gilbert, B. P.; Pelzer, G.; Depauw, E. *Org. Mass Spectrom.* **1986**, *21*, 443−444.

(19) Jaeger, D. A.; Su, D. *Tetrahedron Lett.* **1999**, *40*, 257−260.

(20) (a) Warshel, A.; Levitt, M. *J. Mol. Biol.* **1976**, *103*, 227−249. (b) Kaminski, G. A.; Jorgensen, W. L. *J. Phys. Chem. B* **1998**, *102*, 1787−1796.

(21) Jorgensen, W. L.; Tirado-Rives, J. *J. Comput. Chem.* **2005**, *26*, 1689−1700.

(22) (a) Repasky, M. P.; Chandrasekhar, J.; Jorgensen, W. L. *J. Comput. Chem.* **2002**, *23*, 1601−1622. (b) Tubert-Brohman, I.; Guimarães, C. R. W.; Repasky, M. P.; Jorgensen, W. L. *J. Comput. Chem.* **2003**, *25*, 138−150. (c) Tubert-Brohman, I.; Guimarães, C. R. W.; Jorgensen, W. L. *J. Chem. Theory Comput.* **2005**, *1*, 817−823.

(23) Vayner, G.; Houk, K. N.; Jorgensen, W. L.; Brauman, J. I. *J. Am. Chem. Soc.* **2004**, *126*, 9054−9058.

(24) Acevedo, O.; Jorgensen, W. L. *Org. Lett.* **2004**, *6*, 2881−2884.

(25) Acevedo, O.; Jorgensen, W. L. *J. Am. Chem. Soc.* **2005**, *127*, 8829−8834.

(26) Acevedo, O.; Jorgensen, W. L. *J. Org. Chem.* **2006**, *71*, 4896−4902.

(27) Acevedo, O.; Jorgensen, W. L. *J. Am. Chem. Soc.* **2006**, *128*, 6141−6146.

(28) Jorgensen, W. L.; Chandrasekhar, J.; Madura, J. D.; Impey, W.; Klein, M. L. *J. Chem. Phys.* **1983**, *79*, 926−935.

(29) Jorgensen, W. L.; Ulmschneider, J. P.; Tirado-Rives, J. *J. Phys. Chem. B* **2004**, *108*, 16264−16270.

(30) Canongia, Lopes, J. N.; Deschamps, J.; Padua, A. H. *J. Phys. Chem. B* **2004**, *108*, 2038−2047.

(31) McDonald, N. A.; Jorgensen, W. L. *J. Phys. Chem. B* **1998**, *102*, 8049−8059.

(32) Acevedo, O. Ph.D. Thesis, Duquesne University, Pittsburgh, PA, 2003.

(33) Breneman, C. M.; Wiberg, K. B. *J. Comput. Chem.* **1990**, *11*, 361−373.

(34) Thompson, J. D.; Cramer, C. J.; Truhlar, D. G. *J. Comput. Chem.* **2003**, *24*, 1291−1304.

(35) (a) de Andrade, J.; Böes, E. S.; Stassen, H. *J. Phys. Chem. B* **2002**, *106*, 3546−3548. (b) de Andrade, J.; Böes, E. S.; Stassen, H. *J. Phys. Chem. B* **2002**, *106*, 13344−13351. (c) Margulis, C. J.; Stern, H. A.; Berne, B. J. *J. Phys. Chem. B* **2002**, *106*, 12017−12021. (d) Shah, J. K.; Brennecke, J. F.; Maginn, E. J. *Green Chem.* **2002**, *4*, 112−118. (e) Canongia Lopes, J. N.; Padua, A. H. *J. Phys. Chem. B* **2004**, *108*, 16893−16898. (f) Liu, Z.; Huang, S.; Wang, W. *J. Phys. Chem. B* **2004**, *108*, 12978−12989.

(36) Fannin, A. A., Jr.; Floreani, D. A.; King, L. A.; Landers, J. S.; Piersma, B. J.; Stech, D. J.; Vaughn, R. L.; Wilkes, J. S.; Williams, J. L. *J. Phys. Chem.* **1984**, *88*, 2614−2621.

(37) Shehatta, I. *Thermochim. Acta* **1993**, *213*, 1−10.

(38) *CRC Handbook of Chemistry and Physics*, 52nd ed.

(39) Ruiz-López, M. F.; Assfeld, X.; García, J. I.; Mayoral, J. A.; Salvatella, L. *J. Am. Chem. Soc.* **1993**, *115*, 8780−8787.

(40) Chandrasekhar, J.; Shariffskul, S.; Jorgensen, W. L. *J. Phys. Chem. B* **2002**, *106*, 8078−8085.

(41) Blake, J. F.; Jorgensen, W. L. *J. Am. Chem. Soc.* **1991**, *113*, 7430−7432.

(42) Blake, J. F.; Lim, D.; Jorgensen, W. L. *J. Org. Chem.* **1994**, *59*, 803−805.

(43) Jorgensen, W. L.; Blake, J. F.; Lim, D.; Severance, D. L. *J. Chem. Soc. Faraday Trans.* **1994**, *90*, 1727−1732.

(44) Kong, S.; Evanseck, J. D. *J. Am. Chem. Soc.* **2000**, *122*, 10418−10427.

CT6002753